Environmental Research 285 (2025) 122399

Contents lists available at ScienceDirect

Environmental Research

journal homepage: www.elsevier.com/locate/envres

Assessing the toxicity of traffic-derived air pollution using a primary human air-liquid interface airway *in vitro* model

Gerrit Bredeck [a,1], Tina Wahle [a], Angela A.M. Kämpfer [a], Jochen Dobner [a], A. John F. Boere [b], Paul Fokkens [b], Evert Duistermaat [b], Tim Spannbrucker [a], Andrea Rossi [a], Flemming R. Cassee [b,c], Roel P.F. Schins [a,d,*]

[a] IUF – Leibniz Research Institute for Environmental Medicine, Auf'm Hennekamp 50, 40225 Düsseldorf, Germany
[b] Centre for Sustainability, Environment and Health, National Institute for Public Health and the Environment, PO box 1, Bilthoven, 3720, the Netherlands
[c] Institute for Risk Assessment Sciences (IRAS), Utrecht University, Utrecht, the Netherlands
[d] Department of Pharmacology and Toxicology, Research Institute for Nutrition and Translational Research in Metabolism (NUTRIM), Maastricht University, Maastricht, the Netherlands

ARTICLE INFO

Keywords:
Ambient air pollution
PM2.5
Inter-individual variability
Study design
RNA sequencing

ABSTRACT

Traffic-derived air pollution (TDAP) frequently exceeds the 2021 World Health Organization air quality guideline levels and is linked to respiratory diseases through molecular mechanisms such as oxidative stress and inflammation. To determine these mechanisms without relying on animal models and inter-species extrapolation, physiologically relevant human *in vitro* models are promising tools.

We sought to investigate the oxidative stress and inflammatory responses to TDAP in a co-culture model of the human lung. Additionally, we aimed to examine the variability arising from different exposure days and across primary human *in vitro* models from different donors.

Therefore, primary human bronchial epithelial cultures from three donors, each combined with primary alveolar macrophages, were exposed to a continuous flow of ambient TDAP from a high-traffic street in Düsseldorf, Germany on three consecutive days. A versatile aerosol concentration enrichment system was used to increase the fine particulate matter levels from 8 to 42 μg/cm^2 to 54–143 μg/cm^2.

Gene expression of four oxidative stress markers and four inflammatory cytokines was analyzed by quantitative reverse transcriptase PCR. Compared to incubator controls, even low airflow itself induced the expression of the oxidative stress marker heme oxygenase 1 and the cytokines interleukin 8 and tumor necrosis factor alpha. TDAP exposure, compared to clean air controls, upregulated interleukin 6 in one of the three co-cultures. Because TDAP exposure had minimal effects, exposure day-specific responses could not be discerned. In four of twelve genes, we observe exposure-independet donor differences. Transcriptomic analysis suggested TDAP-induced differential expression of four lung disease-related genes which, however, could not be confirmed by qRT-PCR.

Higher TDAP concentrations or repeated exposures may be required to detect robust effects in this system. Our findings highlight inter-donor variability, underscoring the need for larger donor panels. Future studies should also minimize background effects from airflow to enhance model reliability for real-time TDAP exposure studies.

1. Introduction

Despite attempts to minimize traffic-derived air pollution (TDAP), the World Health Organization (2022) air quality guideline limits are regularly exceeded in urban areas (Lepisto et al., 2023). TDAP consists of solid and gaseous components. The main solid component is particulate matter (PM) with a diameter of less than 1 μm from vehicles with combustion engines (Winijkul et al., 2015). Fine (PM2.5) and coarse (PM10) particulate matter from brake, tire, and road wear also contribute to the cocktail of solid pollutants (Fussell et al., 2022). Additionally, combustion engines emit gaseous toxicants such as nitrogen oxides and volatile organic compounds (Saarikoski et al., 2023).

* Corresponding author. IUF – Leibniz Research Institute for Environmental Medicine, Auf'm Hennekamp 50, 40225 Düsseldorf, Germany.
E-mail address: roel.schins@iuf-duesseldorf.de (R.P.F. Schins).
[1] Present address: Centro de Investigaciones Biológicas Margarita Salas (CIB-CSIC), Madrid, Spain.

https://doi.org/10.1016/j.envres.2025.122399
Received 2 April 2025; Received in revised form 9 July 2025; Accepted 18 July 2025
Available online 5 August 2025

From a long-term perspective, TDAP changes across location and time due to geographical conditions, technological advancements, and the implementation of political regulations (Fowler et al., 2020; Bai et al., 2022). These changes entail the need to continuously reassess the health effects of TDAP. Only a timely understanding of health effects from a molecular to a population-based level can ensure proper regulatory action to protect human health. Many studies have addressed the molecular effects of TDAP using collected and resuspended PM (Chen et al., 2022). However, this approach disregards gaseous compounds and fluctuations in the composition of TDAP.

To achieve more realistic conditions, online exposure systems have been developed to expose rodents or lung *in vitro* models. Sampled air can directly be guided to biological test systems (e.g., Li et al. (2019); Gualtieri et al. (2024)). Additionally, to increase the concentration of PM2.5 by up to 10-fold and facilitate discovering biological effects, Kim et al. (2001) developed the versatile aerosol concentration enrichment system (VACES). The concentration of gaseous compounds remains unaltered in the VACES. The chemical composition as well as the size distribution from 50 nm up to at least 1.9 μm is well-preserved (Kim et al., 2001; Khlystov et al., 2005; Saarikoski et al., 2014), whereas there is a slight decrease in the concentration factor for smaller particles and larger particles that are less relevant for TDAP cannot pass the device. The VACES has already been applied in several mouse exposure studies (Kleinman et al., 2007; Ran et al., 2021). In combination with the VACES, realistic rodent inhalation exposure can be achieved using either a nose-only or whole-body exposure setup. For the exposure of *in vitro* air-liquid interface (ALI) models to aerosols from dynamic sources, devices have been developed that allow subjecting ALI models to a constant airflow (Mülhopt et al., 2016).

Most *in vivo* and *in vitro* studies applying ambient PM2.5 by online exposure address pathways known to be induced by other pulmonary toxicants. In mice, Wan et al. (2010) observed an induced expression of the oxidative stress marker gene heme oxygenase 1 (*HMOX1*), and Li et al. (2019) found inflammatory cytokines, neutrophils, and activated macrophages in the bronchioalveolar lavage fluid. *In vitro*, Volckens et al. (2009) and Gualtieri et al. (2024) analyzed the expression of oxidative stress marker genes *HMOX1* and NAD(P)H dehydrogenase (*NQO1*) and the inflammatory cytokine interleukin 8 (*IL8*), amongst others. To exceed pre-existing hypotheses, Ding et al. (2021) applied RNA-sequencing and discovered that cytochrome P 450 oxidases were involved in oxidative stress induced by ambient PM2.5.

With the drive to replace animal experiments with advanced *in vitro* models, i.e. new approach methodologies (NAMs), a better understanding of molecular mechanisms and the development of realistic *in vitro* models are becoming indispensable (Schmeisser et al., 2023). Considering the abovementioned changes in TDAP composition and the expected associated variability in affected molecular mechanisms, further studies going beyond pre-existing hypotheses are necessary. An important limitation in the development of realistic *in vitro* models assessing the effects of TDAP is that inter-individual differences have barely been addressed. To the best of our knowledge, merely Volckens et al. (2009) used cells from three different donors but did not investigate systematic differences between them. One goal of this study was to evaluate the effect of TDAP in a realistic scenario, applying a hypothesis-driven approach focusing on oxidative stress and inflammation-related gene expression. Simultaneously, we applied a hypothesis-generating approach based on transcriptome-wide RNA sequencing. We also aimed to evaluate the variability in the complex co-culture model and the background effect of exposure in the ALI exposure system.

Here, we used freshly generated TDAP, concentrated the PM2.5 fraction with a VACES, and used a commercially available continuous flow ALI exposure system. We combined primary human bronchial epithelial cells from three donors with primary human alveolar macrophages and exposed each on three consecutive days.

2. Material & methods

2.1. Exposure setup

The *in vitro* exposure study was performed at the IUF – Leibniz Research Institute for Environmental Research in Düsseldorf. *In vitro* exposures were conducted on May 2nd (day 1), May 3rd (day 2), and May 4th (day 3), 2023. Air was drawn into a metal pipe (Ø 10 cm) about 1 m above the ground level. The inlet was situated in a grass field at about 5 m distance from the road. The road comprises two traffic lanes in each direction and two tram lanes in between and is located within the low-emission zone of Düsseldorf that only permits vehicles fulfilling Euro 4 (diesel) or Euro 1 (gasoline) emission standards. The exposure site has an estimated traffic volume of 30,000 vehicles per day. Devices for aerosol sampling, aerosol characterization, particle concentration, and *in vitro* exposure were connected to the other side of the metal pipe with a length of 70 m. The passage time of the aerosol through the metal pipe was calculated to be 82 s and the Reynolds number was 5600. VACES concentrators were used to deliver TDAP to a Vitrocell AES. A schematic diagram of the VACES and the aerosol characterization devices is provided in Figure A1. Four VACES modules were placed in parallel to concentrate PM2.5 in incoming ambient air (400 L/min). The temperature of the VACES humidifiers was adapted to the ambient conditions to reach humidity close to saturation. In this way, the incoming air was saturated with water vapor and subsequently cooled to increase the size of particles before the air was passed through parallel virtual impactors, each operating at 100 L/min. Particles >3 μm mass median aerodynamic diameter were lost by impaction on the walls of the inlet and saturator. Particles with a diameter of about 20 nm or less are not efficiently concentrated by the VACES. The combined output minor flow from the four impactors (10 L/min) was dried in a heated transfer line to restore the original particle state. The negative control in this study was HEPA-filtered clean air from the air-liquid exposure system (Vitrocell, Waldkirch, Germany).

2.2. Characterization of the ambient and in vitro atmospheres

The ambient conditions and the air entering the VACES and the AES were continuously monitored. The meteorological conditions, i.e. temperature, relative humidity, wind direction, and wind speed (Table A1 and Figure A2) were obtained from station 1078 of the German Weather Service. Ambient NO_2 concentrations were obtained from the monitoring station "DENW430 Merowingerstrasse, Düsseldorf" of the "Landesamt für Natur, Umwelt und Verbraucherschutz Nordrhein-Westfalen" located 780 m away from the sampling site. The concentrations of NO and NO_2 before entering the VACES were measured using a Chemiluminescence Nitrogen Oxides Analyzer model 200E (Advanced Pollution Instrumentation T-API, San Diego, CA, USA). Particle numbers entering the VACES and the AES were measured using condensation particle counters (CPC; TSI, Shoreview, MN, USA) model 3022 and model 3752, respectively. On day 1, lawnmowers worked close to the sampling site. This led to peaks in the particle numbers entering the VACES, which exceeded the upper detection limit of the CPC model 3022, resulting in an underestimation of the overall ambient particle count for that day. A scanning mobility particle sizer (U-SMPS DEMC; Palas, Karlsruhe, Germany) combined with a UF CPC 100 (Palas) was used to record the size distributions between 20 nm and 780 nm of the aerosol entering the AES. Per exposure day, six measurements were performed, one per hour. The average PM2.5 concentrations entering VACES and AES on each exposure day were determined gravimetrically using Teflon filters with 2.0 μm pore size and 47 mm diameter (Pall Life Sciences, Port Washington, NY, USA). Before and after particle loading, filters were weighed on a Sartorius ME-5 microbalance after overnight temperature and humidity acclimatization. For the air entering the AES on day 2 and day 3, the gravimetrical measurement was compromised. Instead, PM2.5 concentrations were extrapolated from the particle count

based on data from pilot studies (Figure A3). No quartz crystal microbalance (QCM) was used to measure the deposited dose, because the calculated deposition was about 0.45 ng/cm^2, and thus below the resolution of 10 ng/cm^2 and the lower detection limit of 170 ng/cm^2 of the QCM Cloud 6 microbalance (Ding et al., 2020).

2.3. Cell culture procedure

Primary human bronchial MucilAir cultures on 12-well transwell inserts, frozen primary human alveolar macrophages (AM), and cell culture medium (CCM) for MucilAir cultures were purchased from Epithelix (Archamps, France). MucilAir cultures originated from three different donors, and AM from a fourth donor (Table 1). According to the supplier, all donors were self-reported non-smokers and had no reported pathologies.

After reception, the CCM of MucilAir cultures was changed. After 24 h, the apical side was washed with 300 µL CCM. The cultures were maintained at 37 °C, 5 % CO_2, and saturated humidity for 5, 6, or 7 days, with changes of the basolateral CCM every 2–3 days. Subsequently, 34 µL CCM containing 110,000 unfrozen AM was added onto the apical side of each MucilAir culture. After 24 h, these co-cultures were used for experiments. Hereinafter, they will be referred to as co-culture-A (cc-A), cc-B, and cc-C.

2.4. Exposure procedure

On each exposure day, three of each of the co-cultures were used. One of each co-culture was used as incubator control, one as clean air control, and one for TDAP exposure (Figure A4). Per combination of co-culture, exposure day, and exposure type, a single replicate was used. The AES exposure modules were pre-heated to 37 °C. A leak test ensured no ambient air was drawn to the co-cultures. Wells were filled with 6.5 mL CCM before transferring co-culture inserts to the AES. The exposure modules were closed with the trumpets directing the flow 2 mm above the cells. The co-cultures were exposed at a flow of 5 mL/min for 6 h. The exposure air was humidified to 85 %. After the exposure, co-cultures were transferred to a 12-well plate with fresh CCM for TEER measurement and RNA isolation. The conditioned CCM from the AES was collected for the lactate dehydrogenase (LDH) cytotoxicity assay.

To assess the effect of airflow, incubator controls were handled in parallel. During the exposure time, incubator controls were placed into a 12-well plate with 1.5 mL fresh CCM and kept at 37 °C, 5 % CO_2, and saturated humidity. After the exposure time, the conditioned CCM from incubator controls was collected and diluted to 6.5 mL with fresh CCM.

2.5. LDH assay

To assess cytotoxicity in the co-cultures, the LDH assay was performed. After exposure, 2x50 µL conditioned CCM per sample was transferred to a 96-well plate. The assay was performed as described previously (Busch et al., 2021). The LDH reaction was stopped after 10 min.

2.6. TEER measurement

To assess the barrier integrity, transepithelial electrical resistance (TEER) was measured. To the apical side of co-cultures, 0.5 mL CCM was added, and the plate was allowed to temperature-equilibrate for 1 min. For TEER measurement, an EVOM Volt-ohmmeter with STX2 chopstick electrode (World Precision Instruments, Sarasota, FL, USA) was used. The results were corrected for the blank value of 100 Ω obtained from Epithelix and the transwell area of 1.12 cm^2.

Table 1
Age, sex, and origin of donors.

	Alveolar	MucilAir		
	macrophages	Donor A	Donor B	Donor C
Age	62 years	62 years	15 years	64 years
Sex	Male	Male	Male	Female
Origin	Caucasian	Hispanic	Caucasian	Caucasian

2.7. Targeted gene expression analysis by qRT-PCR

The expression of apurinic/apyrimidinic endonuclease 1/redox effector factor 1 (*APE1/REF1*), C1q and TNF related protein 6 (*C1QTNF6*), gamma glutamate-cysteine ligase (*GGCS*), *HMOX1*, *IL1A*, *IL1B*, *IL6*, *IL8*, lymphotoxin beta (*LTB*), *NQO1*, reticulocalbin 3 (*RCN3*), and tumor necrosis factor alpha (*TNFA*) was assessed by quantitative reverse transcriptase PCR (qRT-PCR). RNA was isolated from co-cultures using the Roche High Pure RNA Isolation kit according to the manufacturer's instructions. As a measure of RNA quality, the ratio of the absorbances at 260 nm and 280 nm was examined. For all except one sample, the ratio was between 2.03 and 2.10. Only for the TDAP-exposed cc-A from Day 3, the ratio was 1.94. For this sample, the RNA Integrity Number (RIN) equivalent was measured and was higher than 7. RNA quantification, DNase I digestion, reverse transcription, and qPCR were performed as described previously (Kampfer et al., 2021). qPCRs were performed on a QuantStudio™ 3 device (Thermo Fisher Scientific, Waltham, MS, USA). The primer pairs are listed in Table A2. C_T values were determined using the QuantStudio™ Design & Analysis Software and corrected for primer efficiencies. Gene expressions are reported as ΔC_T values in comparison to the reference gene actin beta (*ACTB*). *ACTB* was selected as the reference gene due to its low variability in C_T values across all 27 samples, i.e., standard deviation of 0.38.

2.8. Transcriptomics by long-read RNA sequencing

To assess the effect of exposure to TDAP on gene expression more comprehensively and examine the variability between exposure days and co-cultures, RNA sequencing was performed. A total of twelve samples were examined. Per co-culture, the control samples from the three exposure days were pooled. Per co-culture and exposure day, one TDAP exposure sample was assessed (Figure A5). Total RNA was extracted (see 2.7) and RNA integrity was determined using an RNA Screen Tape on a TapeStation 4200 System (Agilent, Santa Clara, CA, USA). RNA with an RIN equivalent $\geq$7 was subjected to double-stranded cDNA (ds-cDNA) synthesis, amplification, and sequencing library preparation. 200 ng of total RNA was subjected to the previously described procedure (Dobner et al., 2024) with the adaption of performing eight cycles of ds-cDNA amplification in duplicate.

2.9. Sequencing data analysis and statistics

Signals derived from long-read sequencing were basecalled using Guppy (version 6.4.6). Subsequently, FASTQ files were mapped to the human reference genome (GRCh38) with Minimap2 (version 2.24). Sequencing reads were counted using Rsubread (version 2.12.3) and normalized to counts per million. Differentially expressed transcripts were identified using edgeR (version 3.40.2) and gene set enrichment analysis was performed using clusterProfiler (version 4.6.2). Graphs and statistical visualizations of sequencing data were created with ggplot2 (version 3.4.2).

LDH release, TEER, and the expression of targeted genes were analyzed with the following statistical methods: The effects of airflow and co-culture were assessed by two-way ANOVAs. Per exposure group, Tukey's post hoc tests were applied to examine differences between co-cultures. The TDAP effect on each exposure day was assessed with paired t-tests with Šidák's correction. When jointly analyzing the three exposure days, the effects of TDAP and co-culture were assessed using repeated measurements two-way ANOVAs with Tukey's multiple comparison tests to examine co-culture differences per exposure group and

exposure effects per co-culture. Šidák's corrections were calculated using R (version 4.4.2). All other statistics and visualizations were performed with GraphPad Prism (version 10.2.0). Statistical significance was inferred at $p \leq 0.05$.

3. Results and discussion

3.1. Exposure conditions

In this study, we translated urban TDAP into realistic *in vitro* exposure. The ambient PM2.5 concentrations of 8–42 μg/m^3 on the three study days (Table A1) were typical for European cities (Lepisto et al., 2023). Using a VACES, particle number concentrations were increased by factors 9.4, 8.0, and 10.1 for *in vitro* exposure resulting in PM2.5 concentrations of 54–143 μg/m^3 (Tables 2 and A3). Although these concentrations substantially exceeded the annual and 24-h WHO air quality guideline values of 5 μg/m^3 and 15 μg/m^3, respectively (World Health Organization, 2022), they were not unrealistic, being frequently reached in highly polluted urban areas (Salo et al., 2021; Goodarzi et al., 2023). Concentrating PM2.5 with the VACES also compensated for experimental underestimations in our model. Firstly, in the AES, only about 1 % of the particles deposit onto the cells (Lucci et al., 2018). In contrast, the deposition of ultrafine and fine particles in the human bronchial region lies between 0.3 % and 9.6 % according to ICRP (1994) and between 3.5 % and 7.6 % according to Lv et al. (2021) depending on particle size as well as a person's age, sex, physical activity, breathing habit and breathing rate. Secondly, the *in vitro* exposure time is limited to 6 h, while TDAP exposure is chronic for people living or working in high-traffic areas.

The 6 h average concentrations of NO and NO_2 were highly similar throughout the three exposure days (Table 2). The NO_2 concentrations did not exceed the annual WHO air quality guideline value of 10 μg/m^3.

Additionally, we recorded time-resolved and size-distribution-resolved concentrations for each exposure day. We observed the highest peaks in particle number concentration during a 15-min time window on day 1 caused by lawnmowing activities with a two-stroke petrol engine close to the sampling site (Figure A6). These peaks were not accompanied by elevated concentrations of nitrogen oxides (Figure A7). Disregarding the period of lawnmowing activities, the highest peaks in particle number concentration and nitrogen oxide concentration were still observed on day 1. Analyzing the size range of 20–780 nm, particles <100 nm were more frequent than particles >100 nm on day 1 but not on days 2 and 3 (Figure A8).

3.2. Effects of airflow

For *in vitro* exposure, we incubated primary human co-cultures of bronchial MucilAir tissue and alveolar macrophages in a Vitrocell AES. To evaluate how airflow exposure in the AES affected cytotoxicity, barrier integrity, oxidative stress, and inflammatory cytokines, we compared clean air controls to the simultaneously cultured incubator controls. After exposure for 6 h, LDH release as a marker for cytotoxicity was not increased in the clean air controls (Fig. 1a). This agrees with studies in primary human bronchial epithelial cells (Volckens et al., 2009), bronchial epithelial 16HBE14o$^-$ cells (Aufderheide et al., 2011), and co-cultures of bronchial epithelial BEAS-2B cells and THP-1 macrophages (Paur et al., 2008).

Table 2
Exposure concentrations of particles and nitrogen oxides.

	Particle count	PM2.5 conc.[a]	NO conc.	NO_2 conc.	NO_x conc.
Day 1	150,687/cm^3	143 μg/m^3	2 μg/m^3	7 μg/m^3	9 μg/m^3
Day 2	42,831/cm^3	[a]54 μg/m^3	2 μg/m^3	7 μg/m^3	9 μg/m^3
Day 3	67,655/cm^3	[a]90 μg/m^3	2 μg/m^3	8 μg/m^3	10 μg/m^3

[a] Mass concentrations were extrapolated from the particle count because of compromised gravimetric measurements.

Meanwhile, elevated TEER indicated increased barrier function (Fig. 1b), which might be related to airflow acting as a mechanical stimulus. Sidhaye et al. (2008) associated mechanical stimulation with the increased expression of tight junctions.

Airflow also increased the expression of the oxidative stress marker gene *HMOX1* by about 2-fold and the expression of the inflammatory cytokines *IL8* and *TNFA* by about 1.5-fold and 3-fold, respectively (Table 3, Figure A9a,g,h). The expression of the oxidative stress marker genes *NQO1*, *APE1/REF1*, and *GGCS* as well as the cytokines *IL1B* and *IL6* was not affected by airflow (Table 3, Fig. 1b–f). In agreement with our results, Paur et al. (2008) observed that airflow slightly increased IL-8 release from BEAS-2B/THP-1 co-cultures. However, they reported no effect on HMOX-1 protein levels. Other studies using similar exposure settings did not include incubator controls (Panas et al., 2014) or merely assessed cytotoxicity (Volckens et al., 2009; Aufderheide et al., 2011).

Additionally, we assessed the variability between co-cultures without and with airflow. Although the constitutive TEER value was about 200 Ω*cm^2 higher in cc-C than in cc-B, we did not observe inherent donor-related differences in gene expression. However, after exposure to airflow in the AES, the *IL6* expression was about 3-fold higher in cc-C than cc-A.

Together, these results reveal that subjecting *in vitro* models to airflow in the complex AES poses oxidative and inflammatory stress which is partly specific for different individuals. This AES-stress may obscure the effects of the toxicants under investigation.

3.3. Effects of TDAP

We assessed the cytotoxicity of TDAP and its effects on barrier integrity and the gene expression of oxidative stress marker genes and pro-inflammatory cytokines. First, we evaluated each exposure day separately and could not detect any effect (Table 4, Fig. 2, A.10, and A.11). Subsequently, we analyzed the data from the three exposure days together to examine co-culture-specific TDAP effects and differences between co-cultures in each exposure group. Merely in cc-B, TDAP exposure induced *IL6* expression by about 2-fold (Figure A11j) indicating inter-individual differences in sensitivity. For *NQO1* expression, there was a statistically significant interaction between co-culture and exposure. However, the post hoc test did not reveal a significant TDAP effect for any of the co-cultures (Figure A10j). Therefore, we must reject the hypothesis that oxidative stress-related genes are induced by TDAP while the effects on pro-inflammatory cytokines are minimal in our exposure scenario.

Previous *in vitro* and *in vivo* studies on ambient PM widely contrast the absence of oxidative and inflammatory effects. PM2.5 from downtown Los Angeles induced oxidative activity in rat alveolar macrophages (Pirhadi et al., 2020a, 2020b). However, the authors exposed submerged cultures to resuspended PM sampled via VACES or electrostatic precipitator. Volckens et al. (2009) observed increased expression of *HMOX1* and *IL8* in primary human bronchial epithelial ALI cultures in response to concentrated coarse ambient PM. In addition to the difference in particle size, their concentration of 2 μg/cm^2 was significantly higher than in our study. In an exposure set-up similar to our study, but without a particle concentration step, Gualtieri et al. (2024) exposed human bronchial BEAS-2B cells to urban PM_1 from Bologna for 24 h. On zero, two, and four of 16 days, they observed a > 2-fold upregulation of *IL8*, *HMOX1,* and *NQO1*, respectively. Wan et al. (2010) exposed mice to VACES-concentrated PM2.5 from Ohio for ten weeks and observed an induction of *HMOX1* expression. Besides the different models, the contrast between our results and those of Gualtieri et al. (2024) and Wan et al. (2010) may be caused by the 4-times and 50-times higher exposure time in their studies, respectively.

Among the TDAP-exposed samples, LDH release was higher for cc-A than cc-C. Among the clean air controls, *APE1/REF1* expression was higher in cc-B than in the other co-cultures. The differences between co-

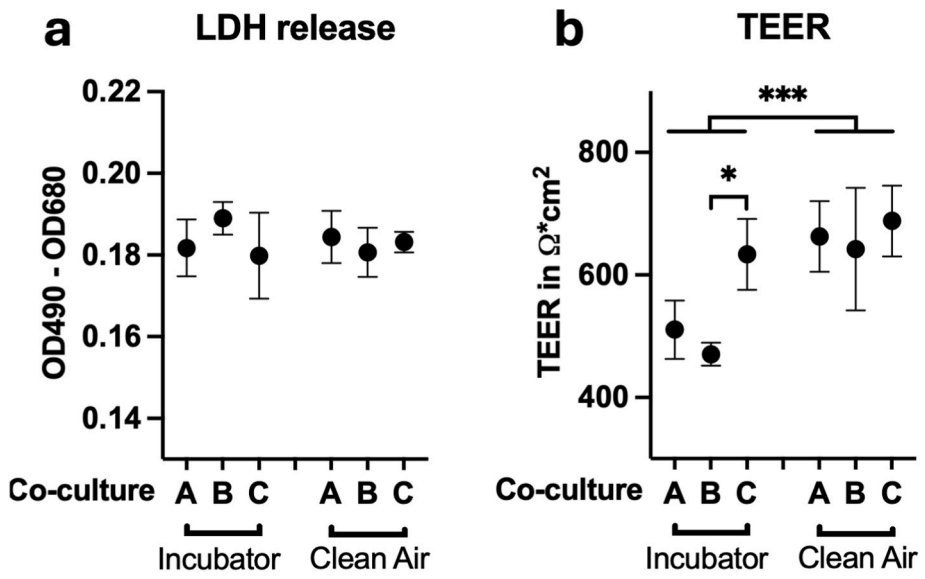

Fig. 1. Effects of airflow. The MucilAir macrophage co-cultures A-C were exposed to airflow for 6 h (Clean Air), while controls were placed back into the incubator. The LDH assay was performed on the basolateral medium (**a**) and TEER was measured (**b**). Two-way ANOVAs were applied to assess the effect of exposure and co-culture. Differences between co-cultures per exposure were analyzed using Tukey's multiple comparison tests (***$p < 0.001$). Abbreviations: LDH, lactate dehydrogenase; OD, optical density; TEER, transepithelial electrical resistance.

Table 3
Effects of airflow on the gene expression of oxidative stress marker and inflammatory cytokines listed as $\log_2$(fold change).

Gene	Incubator				Clean Air			
	cc-A	cc-B	cc-C	Mean ± SD	cc-A	cc-B	cc-C	Mean ± SD
HMOX1	0.00 ± 0.50	0.36 ± 1.25	−0.27 ± 0.28	0.03 ± 0.31	1.23 ± 0.58	1.76 ± 0.29	1.23 ± 0.17	**1.41 ± 0.30*****
NQO1	0.00 ± 0.77	−0.15 ± 0.41	0.25 ± 0.58	0.03 ± 0.20	0.08 ± 0.52	−0.17 ± 0.45	−0.23 ± 0.56	−0.10 ± 0.16
APE1/REF1	0.00 ± 0.78	−0.23 ± 0.32	−0.49 ± 0.24	−0.24 ± 0.25	0.01 ± 0.21	0.28 ± 0.18	−0.10 ± 0.14	0.06 ± 0.20
GGCS	0.00 ± 0.78	−0.08 ± 0.3	−0.28 ± 0.21	−0.12 ± 0.15	−0.06 ± 0.03	0.27 ± 0.33	−0.38 ± 0.29	−0.05 ± 0.32
IL1B	0.00 ± 0.71	0.02 ± 1.00	0.13 ± 0.82	0.05 ± 0.07	1.15 ± 1.64	−0.07 ± 1.00	−0.06 ± 1.02	0.34 ± 0.70
IL6	0.00 ± 0.59	−0.52 ± 0.54	0.45 ± 0.52	−0.02 ± 0.49	**−0.47 ± 0.79**$^{\#\#}$	−0.24 ± 0.14	**1.00 ± 0.69**$^{\#\#}$	0.09 ± 0.79
IL8	0.00 ± 0.45	−0.16 ± 0.25	−0.42 ± 0.12	−0.19 ± 0.21	0.44 ± 0.45	0.45 ± 0.38	0.53 ± 0.55	**0.48 ± 0.05****
TNFA	0.00 ± 0.79	−0.14 ± 1.95	0.67 ± 0.93	0.18 ± 0.43	1.77 ± 1.40	1.29 ± 0.32	2.11 ± 0.98	**1.72 ± 0.41***

Gene expression was measured by qRT-PCR. For each co-culture (cc) mean values of $\log_2$(fold changes) over the incubator control of cc-A were calculated and standard deviations were derived from ΔC_T values. Additionally, mean values with standard deviations (SD) across cc-A, cc-B, and cc-C were calculated. $N = 3$ independent experiments were performed. Two-way ANOVAs were applied to assess the effect of airflow exposure and co-culture and differences between co-cultures per exposure were analyzed using Tukey's multiple comparison tests (*$p < 0.05$, **$p < 0.01$, ***$p < 0.001$ comparing incubator controls to clean air exposed samples; $^{\#\#}p < 0.01$ comparing cc-A and cc-C within the same exposure group; no significant differences between cc-B and any of the other co-cultures obtained).

Table 4
Effects of TDAP exposure on the gene expression of oxidative stress marker and inflammatory cytokines listed as $\log_2$(fold change).

Gene	Day 1				Day 2				Day 3			
	cc-A	cc-B	cc-C	Mean ± SD	cc-A	cc-B	cc-C	Mean ± SD	cc-A	cc-B	cc-C	Mean ± SD
HMOX1	0.42	−0.14	1.69	0.66 ± 0.94	−0.19	0.00	−0.06	−0.08 ± 0.10	0.96	0.84	0.12	0.64 ± 0.45
NQO1	0.22	0.04	0.45	0.24 ± 0.20	0.37	−0.58	0.23	0.01 ± 0.52	0.22	−0.12	0.12	0.07 ± 0.17
APE1/REF1	0.20	−0.16	−0.18	−0.04 ± 0.21	0.11	−0.21	0.18	0.03 ± 0.21	−0.07	−0.12	−0.11	−0.10 ± 0.02
GGCS	0.46	−0.25	0.47	0.23 ± 0.41	0.45	−0.50	0.09	0.01 ± 0.48	0.25	0.22	−0.03	0.14 ± 0.15
IL1B	−1.71	2.09	0.21	0.19 ± 1.90	0.01	2.93	−0.76	0.73 ± 1.94	−1.36	−0.02	0.31	−0.36 ± 0.89
IL6	−0.25	0.88	−0.25	0.13 ± 0.65	0.69	1.20	−0.29	0.53 ± 0.76	0.36	0.50	−0.08	0.26 ± 0.30
IL8	−0.46	0.59	0.32	0.15 ± 0.55	1.23	0.28	0.14	0.55 ± 0.59	0.50	0.32	0.25	0.36 ± 0.13
TNFA	−0.31	0.78	−0.26	0.07 ± 0.62	2.16	0.88	−0.71	0.77 ± 1.44	0.74	1.05	0.63	0.81 ± 0.21

Gene expression was measured by qRT-PCR. The effect of TDAP on each of the exposure days was analyzed separately using a paired *t*-test with Šídák's post hoc correction (no statistical significance was obtained).

cultures we found here differ from those obtained for the same samples when comparing with the incubator controls. To adhere to good scientific practice, we performed the qRT-PCR measurements with the same clean air controls twice, once for direct comparison with incubator controls and once for TDAP exposure samples. Hence, it is not surprising that significances are not consistently reached, considering the relatively small differences between the co-cultures as well as the expected methodological variation and that only the analysis of TDAP exposure demanded a repeated measurement design in the statistical evaluation.

3.4. Effects of TDAP on lung disease-related genes

To generate hypotheses on lung disease-related genes, we globally examined gene expression by transcriptome sequencing. We found that

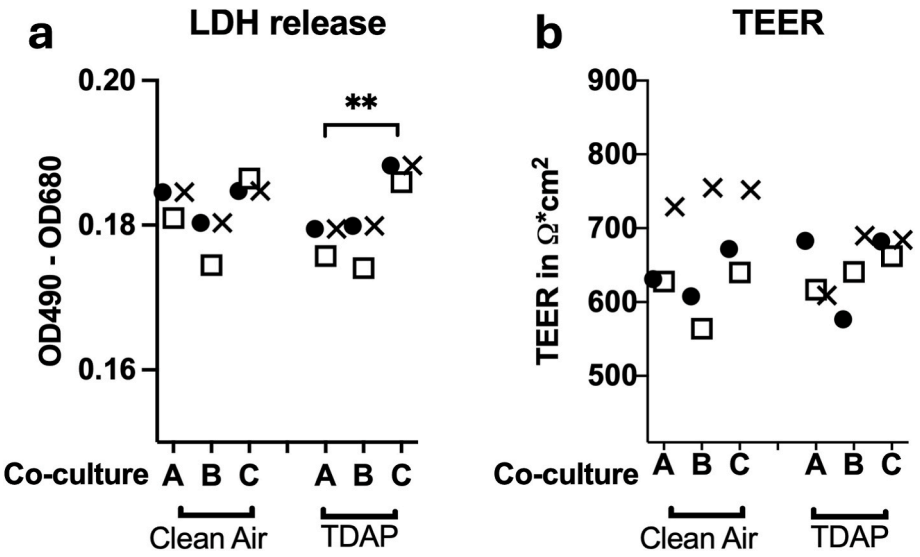

Fig. 2. Effects of TDAP exposure. The MucilAir macrophage co-cultures A-C were exposed to clean air as control and TDAP for 6 h. The LDH assay was performed on the basolateral medium (**a**) and TEER was measured (**b**). The effect of TDAP on each of the exposure days was analyzed separately using a paired *t*-test with Šídák's post hoc correction (no statistical significance was obtained). Additionally, the days were jointly analyzed using a repeated measurement two-way ANOVA to assess the overall effect of TDAP exposure as well as differences between co-cultures per exposure group and exposure effects per co-culture applying Tukey's multiple comparison tests (**$p < 0.01$). Abbreviations: LDH, lactate dehydrogenase; OD, optical density; TEER, transepithelial electrical resistance; TDAP, traffic-derived air pollution.

the lung disease-related genes *IL1A*, *LTB*, *C1QTNF6*, and *RCN3* were differentially expressed in response to TDAP exposure on at least two study days (Table 5). Importantly, all 34 DEGs that were ≥ 4-fold dysregulated on two or three days were either consistently upregulated or downregulated (Table B1).

IL-1α has been shown to drive pulmonary inflammation in response to silica dust (Rabolli et al., 2014) and cigarette smoke (Botelho et al., 2011). LT-β receptor signaling has been connected to the development of severe asthma (Miki et al., 2023). Moreover, LT-β has been shown to be induced in BEAS-2B cells upon exposure to crystalline silica and lipopolysaccharides (Ovrevik et al., 2009). *C1qtnf6* has been reported to be protective against the inflammation induced by the urban particle sample SRM 1649b in mice (Wang et al., 2020). RCN3 has been described to be involved in the transforming growth factor-β1-mediated orchestration of fibroblast activation (Wu et al., 2023) and lipopolysaccharide-induced acute lung injury (Shi et al., 2021), whereas Jin et al. (2018) found that RCN3-deficiency enhanced bleomycin toxicity.

However, we could not corroborate the differential expression of *IL1A, LTB, C1QTNF6,* and *RCN3* by qRT-PCR (Table 6, Figure A11). According to Schurch et al. (2016), the relatively low number of replicates might entail false positive results in the RNA sequencing analysis. The robustness in the direction of the effect detected by RNA sequencing disagreed with the DEGs being merely false positives. Additionally, when a gene was differentially expressed on two of three days according to RNA sequencing, and we analyzed the three days by qRT-PCR, the clean air controls of none of the days systematically deviated from the others. This indicated that pooling the controls from different days is an unlikely reason for obtaining false positive results from RNA sequencing.

The qRT-PCR experiments showed differences between co-cultures in *C1QTNF6* and *LTB* expression among the clean air controls and TDAP exposures, respectively. Analysis of incubator controls indicated that airflow did not obscure TDAP effects on *IL1A, LTB, C1QTNF6,* and *RCN3* (Table A4, Figure A13).

Table 5
Genes ≥ 4-fold dysregulated on at least two exposure days.

Days	Upregulated genes	Downregulated genes
1, 2, and 3	*TMEM225B*, *VIPR2*	*PLP1*
1 and 2	*GPR27*, ***IL1A***, *RGPD1*	*B3GNT8*, *BCAM*, *BEX1*, ***LTB***, POC1B-GALNT4, *RAB3A*, ***RCN3***, *RELL2*, *RUSF1*, *SPNS1*, *SPSB3*, *SRGN*, *SYT8*
1 and 3	***C1QTNF6***, *CD101*, *ETV4*, *GMIP*, *GUCA1B*, *HIC1*, *PAG1*, *TMEM238*, *TNXB*	*ENSG00000241962*, *TYR*
2 and 3	*C17orf67*, *PRR19*	*DIRAS3*, *F2RL2*

3.5. *Variability among exposure days and co-cultures*

Ultimately, we investigated the variability in our exposure setup. Differences between the co-cultures were revealed in the qRT-PCR data. As described above, TDAP only induced *IL6* in one co-culture. The expression of *IL6*, *LTB*, *APE1/REF1*, and *NQO1* differed between co-cultures. The small overlap between the co-cultures regarding DEGs identified by RNA sequencing supported co-culture-specific differences (Figure A14a). Many of the overlapping DEGs were upregulated in one co-culture and downregulated in another (Table B1). However, as discussed above, our RNA sequencing data likely contained false positives which would contribute to the low overlap. To our knowledge, no similar study has been performed assessing air pollution in cultures from different donors by RNA sequencing. Applying qRT-PCR, Bowers et al. (2022) reported 7.0–14.2-fold ranges of the induction of oxidative stress and inflammation-related genes in ozone-exposed primary human bronchial epithelial air-liquid interface cultures from 25 donors. Moreover, Hossain et al. (2022) described high inter-individual differences in air pollution-related health risks among 21 individuals.

The absence of TDAP effects in the targeted gene expression analysis rendered the investigation of exposure day-specific effects based on qRT-PCR impossible. The small overlap in DEGs identified by RNA sequencing (Figure A14b) and the differences in enriched gene sets between the exposure days (Figure A15) suggested high variability between the exposure days. However, the reliability of these results could again be affected by false positive DEGs. In correspondence with variability between exposure days, Volckens et al. (2009) reported high differences in *HMOX1* and cyclooxygenase 1 expression between six

Table 6
Effects of TDAP exposure on the expression of lung disease related genes listed as $\log_2$(fold change).

Gene	Day 1				Day 2				Day 3			
	cc-A	cc-B	cc-C	Mean ± SD	cc-A	cc-B	cc-C	Mean ± SD	cc-A	cc-B	cc-C	Mean ± SD
IL1A	−0.74	1.99	0.36	0.54 ± 1.38	−0.12	2.99	−0.72	0.72 ± 1.99	−1.47	−0.16	0.20	−0.47 ± 0.88
LTB	−1.04	2.65	−1.95	−0.11 ± 2.43	4.28	0.39	−0.39	1.42 ± 2.50	−0.81	−2.97	1.16	−0.87 ± 2.06
C1QTNF6	0.22	−0.77	−1.45	−0.66 ± 0.84	0.45	−1.78	−0.07	−0.47 ± 1.17	0.49	1.26	0.76	0.84 ± 0.39
RCN3	−0.39	0.77	0.18	0.18 ± 0.58	−1.21	−1.16	0.24	−0.71 ± 0.82	0.50	0.07	−0.73	−0.06 ± 0.62

Gene expression was measured by qRT-PCR. For each exposure day, mean values and standard deviations (SD) across cc-A, cc-B, and cc-C were calculated. The effect of TDAP on each of the exposure days was analyzed separately using a paired *t*-test with Šídák's post hoc correction (no statistical significance was obtained).

exposure days. Similarly, Gualtieri et al. (2024) obtained varying differential expressions of seven genes assessed on 16 exposure days. Moreover, Chen et al. (2020) reported variability in the induction of oxidative stress and inflammatory cytokine release in association with the seasonal differences in the composition of PM2.5.

4. Limitations and recommendations

A limitation of our exposure is that the relatively long sampling line and particle concentration in the VACES may have changed the mixture reaching the cells compared to what a subject can inhale at the sampling inlet. The Reynolds number of 5600 indicating turbulent flow as well as the applied flow rate and diameter of the sampling line suggest that minimal losses could be expected for PM2.5. We also cannot rule out that the residence time in the sampling line has resulted in coagulation of compounds or the accumulation of particles by gas-to-particle reactions that may have affected the toxic potency of the aerosol to which the cells were exposed (Kumar et al., 2008). It is unlikely that, apart from ozone, losses of gases have occurred in the sampling line. Moreover, the particle-to-gas ratio shifts due to the enrichment process of the VACES which already changes the composition compared to the ambient condition. The VACES performance also drops below ~20 nm as such small particles do not grow to the size for which the virtual impactors are designed and behave like gas molecules and are neither concentrated nor lost. In contrast to the particle-to-gas ratio, the chemical composition of the particles is not markedly changed when passing an aerosol through the VACES (Freney et al., 2006).

From our data, it is difficult to estimate which exposure day was more hazardous and which co-culture was most sensitive. The additional exposure caused by the lawnmower activity on day 1 in concert with higher PM2.5 concentrations on this day was not reflected in biological effects. The cc-B-specific *IL6* effect and the high number of DEGs in cc-B suggest it is more susceptible to TDAP. However, none of the other investigated genes showed a co-culture-specific TDAP effect in qRT-PCR. While combining different exposure days and co-cultures composed of cells from different donors served our aim to estimate the viability in our complex study design, it limited our ability to detect effects on specific genes.

Focusing on cells from one donor will reduce variability, simplify identifying DEGs, and decrease workload and costs. However, the donor-associated differences in our study showed that such a limitation may introduce substantial bias. Rather, cells from a larger number of donors should be assessed in future studies to increase statistical power. Another option could be to use pooled donors, as has already been applied to nasal cells (Bardet et al., 2016). Potential biases by using cells from a single donor should also be avoided in static systems, i.e., submerged exposure or nebulization of suspended PM. On the other hand, using immortal cell lines improves the comparability between experiments and even offers the possibility to perform large interlaboratory studies. In the future, physiological relevance and broad availability and comparability may be reached by the development of stem cell-based models (Fritsche et al., 2021).

Variable biological effects, as observed for the slightly overlapping DEGs per exposure day, were associated with the TDAP load fluctuating from day to day. Based on this, the coverage of several exposure days significantly increases the value of studies. Instead of single exposure days, repeated exposures over several days may be considered. When attempting repeated *in vitro* exposures, it will be challenging to cope with the risk of contaminating cell cultures with bacteria and fungi or their spores contained in the unfiltered outdoor air.

Moreover, our data also revealed the potential obscuring of results through stress caused by the transfer of ALI cultures from the incubator to altered conditions in the continuous flow exposure system. As in our study, in most studies relying on continuous exposure (Panas et al., 2014; Bowers et al., 2022; Gualtieri et al., 2024), ALI cultures are maintained in an incubator until exposure to a test atmosphere under airflow conditions. Our results show that the switch from incubator to exposure device conditions alone poses a potent stressor. This stressor might alter the reaction of lung cells that should already be physiologically accustomed to airflow. Therefore, future studies should address whether ALI cultures can be preconditioned to airflow by clean air exposures preceding the exposure to the toxicant under investigation. A preconditioning protocol must either be established before starting with exposures, or both unexposed incubator controls and unexposed preconditioned controls must be performed. The comparison of the two controls among each other and with exposures will help distinguish airflow-induced effects from exposure-induced effects.

Another limitation of our study is the restriction to gene expression data. Future studies should validate key findings from RNA sequencing at the protein level, for example, by ELISA, Western blot, or functional assays. Although such validation would require more biological material, it would substantiate the relevance of dysregulated genes.

5. Conclusion

Here, we combine devices for online aerosol characterization, a VACES for aerosol concentration, and a continuous flow ALI exposure system for real-time continuous TDAP exposure of primary human ALI *in vitro* models from multiple donors. Besides the upregulation of *IL6* in one of the three co-cultures, we could not confirm our hypothesis that TDAP induces oxidative stress and inflammatory cytokines in our model. Our approach might serve to generate hypotheses on TDAP-regulated lung disease-related genes such as *IL1A*, *LTB*, *C1QTNF6*, and *RCN3*. However, we could not corroborate these hypotheses by qRT-PCR. Increased concentrations or exposure times may lead to obtaining more robust effects with our experimental approach. Overall, our setup constitutes an important step towards more realistic *in vitro* conditions. However, in contrast to controlled laboratory exposure settings, e.g., diesel exhaust or spark-generators, this model needs further establishment to increase robustness and enable a reasonable application for online exposure.

CRediT authorship contribution statement

Gerrit Bredeck: Writing – original draft, Visualization, Methodology, Investigation, Formal analysis, Data curation, Conceptualization. **Tina Wahle:** Writing – review & editing, Supervision, Project administration, Methodology, Investigation, Conceptualization. **Angela A.M. Kämpfer:** Writing – review & editing, Methodology, Investigation.

Jochen Dobner: Writing – review & editing, Visualization, Software, Formal analysis, Data curation. **A. John F. Boere:** Writing – review & editing, Formal analysis, Data curation. **Paul Fokkens:** Writing – review & editing, Methodology, Investigation. **Evert Duistermaat:** Writing – review & editing, Methodology, Investigation. **Tim Spannbrucker:** Writing – review & editing, Methodology. **Andrea Rossi:** Writing – review & editing, Supervision, Methodology. **Flemming R. Cassee:** Writing – review & editing, Supervision, Resources, Funding acquisition, Conceptualization. **Roel P.F. Schins:** Writing – review & editing, Supervision, Resources, Funding acquisition, Conceptualization.

Declaration of competing interest

The authors declare that they have no known competing financial interests or personal relationships that could have appeared to influence the work reported in this paper.

Acknowledgments

This project has received funding from the European Union's Horizon 2020 research and innovation programme under grant agreement no. 814978 (TUBE). The IUF is funded by the German federal and state governments - the Ministry of Culture and Science of North Rhine-Westphalia (MKW) and the Federal Ministry of Research, Technology and Space (BMFTR).

The authors would like to thank Isabelle Masson and Jessica Vossen for their support with the *in vitro* exposure experiments. The authors would also like to express their gratitude to Klaus Unfried and Catrin Albrecht for their support with logistics and their considerations regarding the design of the exposure set-up. Furthermore, the authors would like to thank the technical department of the IUF for their support with the adaption and assembly of the exposure set-up.

Appendix A. Supplementary data

Supplementary data to this article can be found online at https://doi.org/10.1016/j.envres.2025.122399.

Data availability

The sequencing data have been deposited in the sequence read archive (SRA) (PRJNA1221473). Further raw data underlying this study are available from the authors upon reasonable request.

References

Aufderheide, M., Scheffler, S., Möhle, N., Halter, B., Hochrainer, D., 2011. Analytical in vitro approach for studying cyto- and genotoxic effects of particulate airborne material. Anal. Bioanal. Chem. 401, 3213–3220. https://doi.org/10.1007/s00216-011-5163-4.

Bai, X., Chen, H., Oliver, B.G., 2022. The health effects of traffic-related air pollution: a review focused the health effects of going green. Chemosphere 289, 133082. https://doi.org/10.1016/j.chemosphere.2021.133082.

Bardet, G., Mignon, V., Momas, I., Achard, S., Seta, N., 2016. Human reconstituted nasal epithelium, a promising in vitro model to assess impacts of environmental complex mixtures. Toxicol. Vitro 32, 55–62. https://doi.org/10.1016/j.tiv.2015.11.019.

Botelho, F.M., Bauer, C.M., Finch, D., Nikota, J.K., Zavitz, C.C., Kelly, A., Lambert, K.N., Piper, S., Foster, M.L., Goldring, J.J., Wedzicha, J.A., Bassett, J., Bramson, J., Iwakura, Y., Sleeman, M., Kolbeck, R., Coyle, A.J., Humbles, A.A., Stampfli, M.R., 2011. IL-1alpha/IL-1R1 expression in chronic obstructive pulmonary disease and mechanistic relevance to smoke-induced neutrophilia in mice. PLoS One 6, e28457. https://doi.org/10.1371/journal.pone.0028457.

Bowers, E.C., Martin, E.M., Jarabek, A.M., Morgan, D.S., Smith, H.J., Dailey, L.A., Aungst, E.R., Diaz-Sanchez, D., McCullough, S.D., 2022. Ozone responsive gene expression as a model for describing repeat exposure response trajectories and interindividual toxicodynamic variability in vitro. Toxicol. Sci. 185, 38–49. https://doi.org/10.1093/toxsci/kfab128.

Busch, M., Bredeck, G., Kampfer, A.A.M., Schins, R.P.F., 2021. Investigations of acute effects of polystyrene and polyvinyl chloride micro- and nanoplastics in an advanced in vitro triple culture model of the healthy and inflamed intestine. Environ. Res. 193, 110536. https://doi.org/10.1016/j.envres.2020.110536.

Chen, H., Oliver, B.G., Pant, A., Olivera, A., Poronnik, P., Pollock, C.A., Saad, S., 2022. Effects of air pollution on human health - mechanistic evidence suggested by in vitro and in vivo modelling. Environ. Res. 212, 113378. https://doi.org/10.1016/j.envres.2022.113378.

Chen, S., Li, D., Wu, X., Chen, L., Zhang, B., Tan, Y., Yu, D., Niu, Y., Duan, H., Li, Q., Chen, R., Aschner, M., Zheng, Y., Chen, W., 2020. Application of cell-based biological bioassays for health risk assessment of PM2.5 exposure in three megacities, China. Environ. Int. 139, 105703. https://doi.org/10.1016/j.envint.2020.105703.

Ding, H., Jiang, M., Li, D., Zhao, Y., Yu, D., Zhang, R., Chen, W., Pi, J., Chen, R., Cui, L., Zheng, Y., Piao, J., 2021. Effects of real-ambient PM(2.5) exposure on lung damage modulated by Nrf2. Front. Pharmacol. 12, 662664. https://doi.org/10.3389/fphar.2021.662664.

Ding, Y., Weindl, P., Lenz, A.G., Mayer, P., Krebs, T., Schmid, O., 2020. Quartz crystal microbalances (QCM) are suitable for real-time dosimetry in nanotoxicological studies using VITROCELL®Cloud cell exposure systems. Part. Fibre Toxicol. 17, 44. https://doi.org/10.1186/s12989-020-00376-w.

Dobner, J., Diecke, S., Krutmann, J., Prigione, A., Rossi, A., 2024. Reassessment of marker genes in human induced pluripotent stem cells for enhanced quality control. Nat. Commun. 15, 8547. https://doi.org/10.1038/s41467-024-52922-1.

Fowler, D., Brimblecombe, P., Burrows, J., Heal, M.R., Grennfelt, P., Stevenson, D.S., Jowett, A., Nemitz, E., Coyle, M., Lui, X., Chang, Y., Fuller, G.W., Sutton, M.A., Klimont, Z., Unsworth, M.H., Vieno, M., 2020. A chronology of global air quality. Philos. Trans. A Math. Phys. Eng. Sci. 378, 20190314. https://doi.org/10.1098/rsta.2019.0314.

Freney, E.J., Heal, M.R., Donovan, R.J., Mills, N.L., Donaldson, K., Newby, D.E., Fokkens, P.H., Cassee, F.R., 2006. A single-particle characterization of a Mobile versatile aerosol concentration enrichment system for exposure studies. Part. Fibre Toxicol. 3, 8. https://doi.org/10.1186/1743-8977-3-8.

Fritsche, E., Haarmann-Stemmann, T., Kapr, J., Galanjuk, S., Hartmann, J., Mertens, P.R., Kampfer, A.A.M., Schins, R.P.F., Tigges, J., Koch, K., 2021. Stem cells for next level toxicity testing in the 21st century. Small 17, e2006252. https://doi.org/10.1002/smll.202006252.

Fussell, J.C., Franklin, M., Green, D.C., Gustafsson, M., Harrison, R.M., Hicks, W., Kelly, F.J., Kishta, F., Miller, M.R., Mudway, I.S., Oroumiyeh, F., Selley, L., Wang, M., Zhu, Y., 2022. A review of road traffic-derived non-exhaust particles: emissions, physicochemical characteristics, health risks, and mitigation measures. Environ. Sci. Technol. 56, 6813–6835. https://doi.org/10.1021/acs.est.2c01072.

Goodarzi, B., Azimi Mohammadabadi, M., Jafari, A.J., Gholami, M., Kermani, M., Assarehzadegan, M.A., Shahsavani, A., 2023. Investigating PM(2.5) toxicity in highly polluted urban and industrial areas in the Middle East: human health risk assessment and spatial distribution. Sci. Rep. 13, 17858. https://doi.org/10.1038/s41598-023-45052-z.

Gualtieri, M., Melzi, G., Costabile, F., Stracquadanio, M., La Torretta, T., Di Iulio, G., Petralia, E., Rinaldi, M., Paglione, M., Decesari, S., Mantecca, P., Corsini, E., 2024. On the dose-response association of fine and ultrafine particles in an urban atmosphere: toxicological outcomes on bronchial cells at realistic doses of exposure at the air liquid interface. Chemosphere 366, 143417. https://doi.org/10.1016/j.chemosphere.2024.143417.

Hossain, S., Che, W., Lau, A.K., 2022. Inter- and intra-individual variability of personal health risk of combined particle and gaseous pollutants across selected urban microenvironments. Int J Environ Res Public Health 19. https://doi.org/10.3390/ijerph19010565.

ICRP, 1994. Human respiratory tract model for radiological protection: ICRP publication 66. Ann. ICRP 24, 1–482.

Jin, J., Shi, X., Li, Y., Zhang, Q., Guo, Y., Li, C., Tan, P., Fang, Q., Ma, Y., Ma, R.Z., 2018. Reticulocalbin 3 deficiency in alveolar epithelium exacerbated bleomycin-induced pulmonary fibrosis. Am. J. Respir. Cell Mol. Biol. 59, 320–333. https://doi.org/10.1165/rcmb.2017-0347OC.

Kampfer, A.A.M., Busch, M., Buttner, V., Bredeck, G., Stahlmecke, B., Hellack, B., Masson, I., Sofranko, A., Albrecht, C., Schins, R.P.F., 2021. Model complexity as determining factor for in vitro nanosafety studies: effects of silver and titanium dioxide nanomaterials in intestinal models. Small 17, e2004223. https://doi.org/10.1002/smll.202004223.

Khlystov, A., Zhang, Q., Jimenez, J.L., Stanier, C., Pandis, S.N., Canagaratna, M.R., Fine, P., Misra, C., Sioutas, C., 2005. In situ concentration of semi-volatile aerosol using water-condensation technology. J. Aerosol Sci. 36, 866–880. https://doi.org/10.1016/j.jaerosci.2004.11.005.

Kim, S., Jaques, P.A., Chang, M., Froines, J.R., Sioutas, C., 2001. Versatile aerosol concentration enrichment system (VACES) for simultaneous in vivo and in vitro evaluation of toxic effects of ultrafine, fine and coarse ambient particles Part I: development and laboratory characterization. J. Aerosol Sci. 32, 1281–1297. https://doi.org/10.1016/s0021-8502(01)00057-x.

Kleinman, M.T., Sioutas, C., Froines, J.R., Fanning, E., Hamade, A., Mendez, L., Meacher, D., Oldham, M., 2007. Inhalation of concentrated ambient particulate matter near a heavily trafficked road stimulates antigen-induced airway responses in mice. Inhal. Toxicol. 19 (Suppl. 1), 117–126. https://doi.org/10.1080/08958370701495345.

Kumar, P., Fennell, P., Symonds, J., Britter, R., 2008. Treatment of losses of ultrafine aerosol particles in long sampling tubes during ambient measurements. Atmos. Environ. 42, 8819–8826. https://doi.org/10.1016/j.atmosenv.2008.09.003.

Lepisto, T., Lintusaari, H., Oudin, A., Barreira, L.M.F., Niemi, J.V., Karjalainen, P., Salo, L., Silvonen, V., Markkula, L., Hoivala, J., Marjanen, P., Martikainen, S., Aurela, M., Reyes, F.R., Oyola, P., Kuuluvainen, H., Manninen, H.E., Schins, R.P.F., Vojtisek-Lom, M., Ondracek, J., Topinka, J., Timonen, H., Jalava, P., Saarikoski, S., Ronkko, T., 2023. Particle lung deposited surface area (LDSA(al)) size distributions

in different urban environments and geographical regions: towards understanding of the PM(2.5) dose-response. Environ. Int. 180, 108224. https://doi.org/10.1016/j.envint.2023.108224.

Li, D., Zhang, R., Cui, L., Chu, C., Zhang, H., Sun, H., Luo, J., Zhou, L., Chen, L., Cui, J., Chen, S., Mai, B., Chen, S., Yu, J., Cai, Z., Zhang, J., Jiang, Y., Aschner, M., Chen, R., Zheng, Y., Chen, W., 2019. Multiple organ injury in male C57BL/6J mice exposed to ambient particulate matter in a real-ambient PM exposure system in Shijiazhuang, China. Environ. Pollut. 248, 874–887. https://doi.org/10.1016/j.envpol.2019.02.097.

Lucci, F., Castro, N.D., Rostami, A.A., Oldham, M.J., Hoeng, J., Pithawalla, Y.B., Kuczaj, A.K., 2018. Characterization and modeling of aerosol deposition in vitrocell® exposure systems - exposure well chamber deposition efficiency. J. Aerosol Sci. 123, 141–160. https://doi.org/10.1016/j.jaerosci.2018.06.015.

Lv, H., Li, H., Qiu, Z., Zhang, F., Song, J., 2021. Assessment of pedestrian exposure and deposition of PM10, PM2.5 and ultrafine particles at an urban roadside: a case study of Xi'an, China. Atmos. Pollut. Res. 12, 112–121. https://doi.org/10.1016/j.apr.2021.02.018.

Miki, H., Kiosses, W.B., Manresa, M.C., Gupta, R.K., Sethi, G.S., Herro, R., Da Silva Antunes, R., Dutta, P., Miller, M., Fung, K., Chawla, A., Dobaczewska, K., Ay, F., Broide, D.H., Tumanov, A.V., Croft, M., 2023. Lymphotoxin beta receptor signaling directly controls airway smooth muscle deregulation and asthmatic lung dysfunction. J. Allergy Clin. Immunol. 151, 976–990 e975. https://doi.org/10.1016/j.jaci.2022.11.016.

Mülhopt, S., Dilger, M., Diabaté, S., Schlager, C., Krebs, T., Zimmermann, R., Buters, J., Oeder, S., Wäscher, T., Weiss, C., Paur, H.-R., 2016. Toxicity testing of combustion aerosols at the air–liquid interface with a self-contained and easy-to-use exposure system. J. Aerosol Sci. 96, 38–55. https://doi.org/10.1016/j.jaerosci.2016.02.005.

Ovrevik, J., Lag, M., Holme, J.A., Schwarze, P.E., Refsnes, M., 2009. Cytokine and chemokine expression patterns in lung epithelial cells exposed to components characteristic of particulate air pollution. Toxicology 259, 46–53. https://doi.org/10.1016/j.tox.2009.01.028.

Panas, A., Comouth, A., Saathoff, H., Leisner, T., Al-Rawi, M., Simon, M., Seemann, G., Dossel, O., Mulhopt, S., Paur, H.R., Fritsch-Decker, S., Weiss, C., Diabate, S., 2014. Silica nanoparticles are less toxic to human lung cells when deposited at the air-liquid interface compared to conventional submerged exposure. Beilstein J. Nanotechnol. 5, 1590–1602. https://doi.org/10.3762/bjnano.5.171.

Paur, H.R., Mülhopt, S., Weiss, C., Diabaté, S., 2008. In vitro exposure systems and bioassays for the assessment of toxicity of nanoparticles to the human lung. Journal für Verbraucherschutz und Lebensmittelsicherheit 3, 319–329. https://doi.org/10.1007/s00003-008-0356-2.

Pirhadi, M., Mousavi, A., Sioutas, C., 2020a. Evaluation of a high flow rate electrostatic precipitator (ESP) as a particulate matter (PM) collector for toxicity studies. Sci. Total Environ. 739, 140060. https://doi.org/10.1016/j.scitotenv.2020.140060.

Pirhadi, M., Mousavi, A., Taghvaee, S., Shafer, M.M., Sioutas, C., 2020b. Semi-volatile components of PM(2.5) in an urban environment: volatility profiles and associated oxidative potential. Atmos. Environ. 223. https://doi.org/10.1016/j.atmosenv.2019.117197.

Rabolli, V., Badissi, A.A., Devosse, R., Uwambayinema, F., Yakoub, Y., Palmai-Pallag, M., Lebrun, A., De Gussem, V., Couillin, I., Ryffel, B., Marbaix, E., Lison, D., Huaux, F., 2014. The alarmin IL-1alpha is a master cytokine in acute lung inflammation induced by silica micro- and nanoparticles. Part. Fibre Toxicol. 11, 69. https://doi.org/10.1186/s12989-014-0069-x.

Ran, Z., An, Y., Zhou, J., Yang, J., Zhang, Y., Yang, J., Wang, L., Li, X., Lu, D., Zhong, J., Song, H., Qin, X., Li, R., 2021. Subchronic exposure to concentrated ambient PM2.5 perturbs gut and lung microbiota as well as metabolic profiles in mice. Environ. Pollut. 272. https://doi.org/10.1016/j.envpol.2020.115987.

Saarikoski, S., Carbone, S., Cubison, M.J., Hillamo, R., Keronen, P., Sioutas, C., Worsnop, D.R., Jimenez, J.L., 2014. Evaluation of the performance of a particle concentrator for online instrumentation. Atmos. Meas. Tech. 7, 2121–2135. https://doi.org/10.5194/amt-7-2121-2014.

Saarikoski, S., Hellén, H., Praplan, A.P., Schallhart, S., Clusius, P., Niemi, J.V., Kousa, A., Tykkä, T., Kouznetsov, R., Aurela, M., Salo, L., Rönkkö, T., Barreira, L.M.F., Pirjola, L., Timonen, H., 2023. Characterization of volatile organic compounds and submicron organic aerosol in a traffic environment. Atmos. Chem. Phys. 23, 2963–2982. https://doi.org/10.5194/acp-23-2963-2023.

Salo, L., Hyvärinen, A., Jalava, P., Teinilä, K., Hooda, R.K., Datta, A., Saarikoski, S., Lintusaari, H., Lepistö, T., Martikainen, S., Rostedt, A., Sharma, V.P., Rahman, M.H., Subudhi, S., Asmi, E., Niemi, J.V., Lihavainen, H., Lal, B., Keskinen, J., Kuuluvainen, H., Timonen, H., Rönkkö, T., 2021. The characteristics and size of lung-depositing particles vary significantly between high and low pollution traffic environments. Atmos. Environ. 255. https://doi.org/10.1016/j.atmosenv.2021.118421.

Schmeisser, S., Miccoli, A., von Bergen, M., Berggren, E., Braeuning, A., Busch, W., Desaintes, C., Gourmelon, A., Grafstrom, R., Harrill, J., Hartung, T., Herzler, M., Kass, G.E.N., Kleinstreuer, N., Leist, M., Luijten, M., Marx-Stoelting, P., Poetz, O., van Ravenzwaay, B., Roggeband, R., Rogiers, V., Roth, A., Sanders, P., Thomas, R.S., Marie Vinggaard, A., Vinken, M., van de Water, B., Luch, A., Tralau, T., 2023. New approach methodologies in human regulatory toxicology - not if, but how and when. Environ. Int. 178, 108082. https://doi.org/10.1016/j.envint.2023.108082.

Schurch, N.J., Schofield, P., Gierlinski, M., Cole, C., Sherstnev, A., Singh, V., Wrobel, N., Gharbi, K., Simpson, G.G., Owen-Hughes, T., Blaxter, M., Barton, G.J., 2016. How many biological replicates are needed in an RNA-seq experiment and which differential expression tool should you use? RNA 22, 839–851. https://doi.org/10.1261/rna.053959.115.

Shi, X., An, X., Yang, L., Wu, Z., Zan, D., Li, Z., Pang, B., Chen, Y., Li, J., Tan, P., Ma, R.Z., Fang, Q., Ma, Y., Jin, J., 2021. Reticulocalbin 3 deficiency in alveolar epithelium attenuated LPS-induced ALI via NF-kappaB signaling. Am. J. Physiol. Lung Cell. Mol. Physiol. 320, L627–L639. https://doi.org/10.1152/ajplung.00526.2020.

Sidhaye, V.K., Schweitzer, K.S., Caterina, M.J., Shimoda, L., King, L.S., 2008. Shear stress regulates aquaporin-5 and airway epithelial barrier function. Proc. Natl. Acad. Sci. U. S. A. 105, 3345–3350. https://doi.org/10.1073/pnas.0712287105.

Volckens, J., Dailey, L., Walters, G., Devlin, R.B., 2009. Direct particle-to-cell deposition of coarse ambient particulate matter increases the production of inflammatory mediators from cultured human airway epithelial cells. Environ. Sci. Technol. 43, 4595–4599. https://doi.org/10.1021/es900698a.

Wan, G., Rajagopalan, S., Sun, Q., Zhang, K., 2010. Real-world exposure of airborne particulate matter triggers oxidative stress in an animal model. Int J Physiol Pathophysiol Pharmacol 2, 64–68.

Wang, J., Zhu, M., Ye, L., Chen, C., She, J., Song, Y., 2020. MiR-29b-3p promotes particulate matter-induced inflammatory responses by regulating the C1QTNF6/AMPK pathway. Aging (Albany NY) 12, 1141–1158. https://doi.org/10.18632/aging.102672.

Winijkul, E., Yan, F., Lu, Z., Streets, D.G., Bond, T.C., Zhao, Y., 2015. Size-resolved global emission inventory of primary particulate matter from energy-related combustion sources. Atmos. Environ. 107, 137–147. https://doi.org/10.1016/j.atmosenv.2015.02.037.

World Health Organization, 2022. Ambient (outdoor) air pollution. https://www.who.int/news-room/fact-sheets/detail/ambient-(outdoor)-air-quality-and-health. (Accessed 3 October 2023).

Wu, M., Wang, Z., Shi, X., Zan, D., Chen, H., Yang, S., Ding, F., Yang, L., Tan, P., Ma, R.Z., Wang, J., Ma, L., Ma, Y., Jin, J., 2023. TGFbeta1-RCN3-TGFBR1 loop facilitates pulmonary fibrosis by orchestrating fibroblast activation. Respir. Res. 24, 222. https://doi.org/10.1186/s12931-023-02533-z.